



# Seismic geomorphology and depositional evolution of the Paleogene Shahejie Formation, Central-North Dongying Depression, Bohai Bay Basin, China

Hongchao Zhao<sup>1,2</sup> · Xiaomin Zhu<sup>1,2</sup> · Shifa Zhu<sup>1,2</sup> · Xiaoxu Wang<sup>1,2</sup> · Fang Zhao<sup>1,2</sup> · Mo Shen<sup>1,2</sup> · Tong Xu<sup>1,2</sup> · Wenpeng Lu<sup>3</sup> · Huili Zhang<sup>3</sup>

Received: 4 July 2018 / Accepted: 30 November 2018 / Published online: 6 January 2019

© Saudi Society for Geosciences 2019

## Abstract

The main objective of this article is to demonstrate the utility of stratal slice images for exploring the sequence stratigraphy and sedimentology of complex depositional systems. The Dongying Depression is underlain by a productive, petroleum-prone, non-marine Cenozoic stratigraphic section. Here, we have integrated the recent 3D seismic profiles and borehole data to map sediment dispersal characteristics of the second member of the Shahejie Formation in the central-north Dongying Depression, located in the Bohai Bay Basin, China. We have documented the following key points: (i) the main strata under study were divided into two long-term sequence cycles (LSC1–2) with 14 middle-term sequence cycles (MSC1–14); (ii) five microfacies, distributary channel, inter-channel, mouth bar, underwater distributary channel, and tributary bay, were identified from well-based analysis of sedimentary facies; (iii) the mouth bar was generated at the center of the study area during the deposit stage of MSC6–7; (iv) the channel was distributed along the EW direction. The seismic sedimentological study on the second member of the Shahejie Formation in this study area highlights the distribution of the most important potential reservoirs.

**Keywords** Seismic geomorphology · Stratal slice · Dongying depression · The second member of the Shahejie Formation · High-resolution stratigraphy · Depositional evolution

## Introduction

The Bohai Bay Basin, located in the eastern portion of North China Craton, contains substantial oil and gas resources (Fig. 1A). During the Cenozoic Era, the Bohai Bay Basin underwent four distinct phases of riftings and subsidences (Allen et al. 1997; Lin et al. 2003; Feng et al. 2013). The Bohai Bay Basin consists of six sub-basins (Liaohe Sub-basin, Bozhong Sub-ba-

sin, Jiyang Sub-basin, Huanghua Sub-basin, Jizhong Sub-basin, Dongpu Sub-basin), four main uplift (Chengning Uplift, Cangxian Uplift, Xingheng Uplift, Neihuang Uplift), and several sags. The Dongying Depression is a relatively independent secondary structural unit of the Jiyang Sub-basin. Its area is approximately 5800 km<sup>2</sup> (with 90-km axial length and 65-km width). And the Dongying Depression, a NE-SW half graben, is bounded by Chenjiazhuang Rise, Qingtuozi Rise, Guangrao Rise, Luxi Uplift, Qingchengshan Rise, and Binxian (Fig. 1A).

Exploration of the Dongying Depression began in 1956. In 1961, the first oil producing well, H8, was completed, which confirmed that there were thick layers of source rocks. In 1962, a high-productivity reservoir was found in the Y2 well, and the Shengli Oil Field began to be developed ever since then. After more than 50 years of exploration and development, numerous structural traps have been found but exploration of lithostratigraphic petroleum reservoir has remained relatively inadequate (Xie et al. 2001).

✉ Hongchao Zhao  
1195545724@qq.com

<sup>1</sup> State Key Laboratory of Petroleum Resources and Prospecting, China University of Petroleum, Beijing 102249, China

<sup>2</sup> College of Geosciences, China University of Petroleum, Beijing 102249, China

<sup>3</sup> Shengli Oilfield Company, SINOPEC, Dongying 257000, Shandong, China

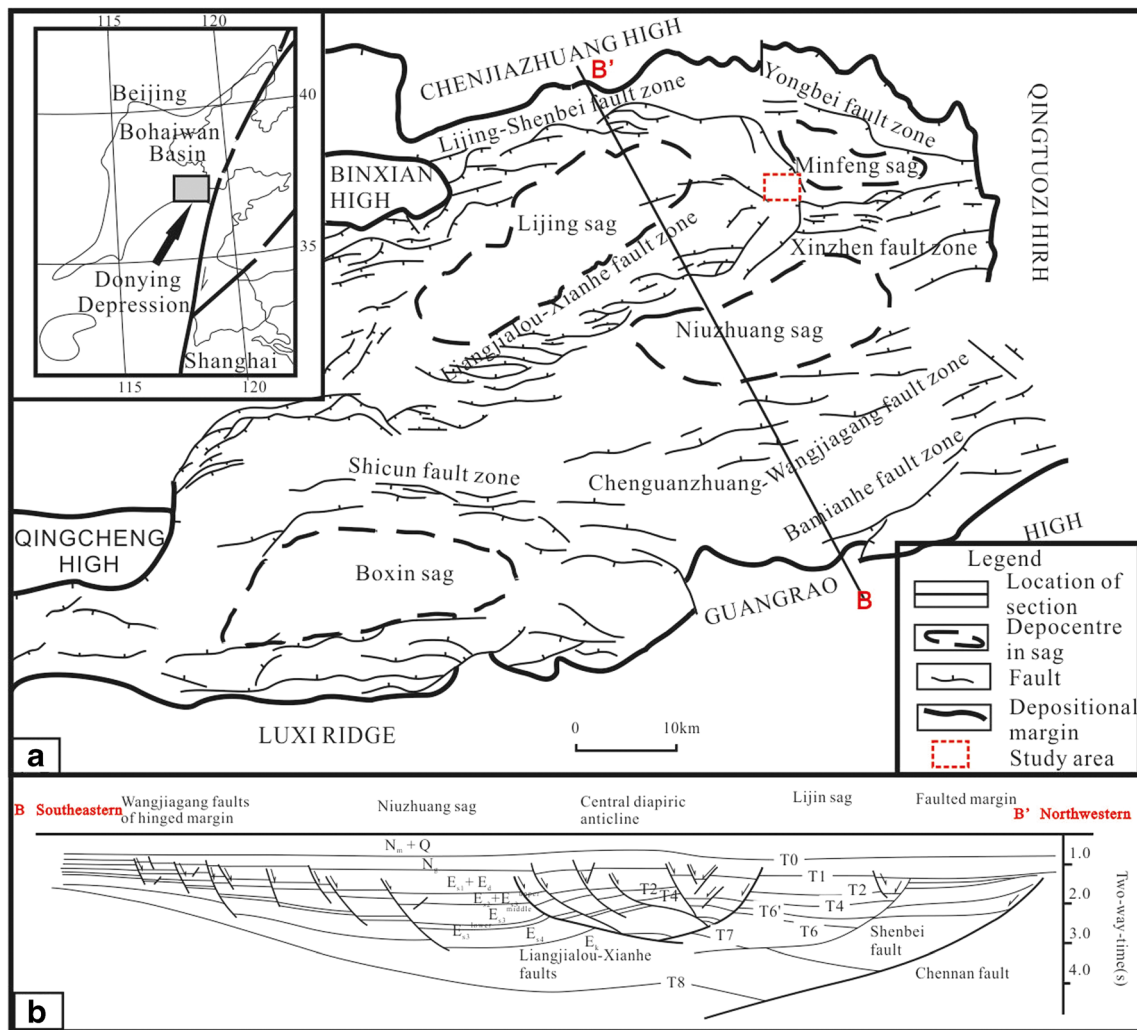


**Fig. 1** Tectonic location map of the Dongying Depression, Bohai Bay Basin, China (A) and tectonic cross-section (B). It indicates the major structural units and tectonic evolution of Dongying Depression (after Xie et al. 2001)

Several previous studies have confirmed the sequence stratigraphy and sedimentary facies of the Dongying Depression (Zong et al. 1999). However, the previous studies have not quantified the shapes, boundaries, distribution, and evolution of the thin-bedded sand bodies which are believed to provide opportunities in the basin. The ability to fully identify bedded reservoirs is a problem when the work is relying only on several drilled wells and conventional seismic data.

Seismic geomorphology can reveal the subtle sedimentology of sands and help demonstrate subtle stratigraphic traps (Dong et al. 2014; Curry et al. 2018; Smit et al. 2018). The objectives of this study are as follows: (i) identifying the sedimentary facies characteristics in the study area, (ii) constructing a high-resolution 3D sequence stratigraphic framework, (iii) defining general sedimentary systems with various middle-term sequence cycles, and (iv) generating sequence stratigraphic and sedimentary models to make a prediction of favorable potential areas for further exploration.

### Data and methodology

In the central-north Dongying Depression, the wellbore control capacity is strong, and more than 400 wells have penetrated the study interval. Moreover, conventional cores from 276 wells provide valuable evidence of sedimentology.

Post-stack-3D seismic data volumes are characterized by an effective frequency range of 10–100 Hz, with a predominant frequency of about 30 Hz. Furthermore, an excellent well-to-seismic tie is obtained using synthetic seismograms from 200 wells. Basically, the Geoscope software is great for interpreting 3D seismic data volumes and generating stratal slices, combined with Petrel 2015 software. The calculated seismic resolution limit (1/4 wavelength of 30 Hz wavelet, with an average velocity of about 3400 m/s) is 25 m. With a good amplitude-thickness relation, a sandbody as thin as 6 m (about 1/6 wavelength) can be detected on a horizontal seismic amplitude (Dong et al. 2015).

Seismic lithology and seismic geomorphology compose the backbone of seismic sedimentology. By applying seismic lithology, we convert a 3D seismic data volume into a lithology data volume. And in a lithology data volume, lithology logs (e.g., GR and SP) are combined with nearby seismic traces within a small tolerance, ensuring the best possible wells integration with seismic data at the reservoir level (Zeng and Hentz 2004). Here, we observe and then describe three important core holes for lithology, respectively namely X16, X49, and X98 with 240 m of the whole description length. Also, we collected the logs data from 276 wells for analysis. For example, the medium-to-high amplitude SP curve can be interpreted as sandstone, and the straight-to-low amplitude SP curve represents mudstone. The CAL curve is related to the well diameter, because the collapsed mudstone has caused larger well diameter. Furthermore, the AC curve can be used to generate the synthetic seismogram, which is a bridge connecting lithology data volume with seismic data volume. After single wells' interpretation, we interpret the well-tie profiles. Based on sedimentary facies environment, several crossed profiles (e.g., AB and CD cross-section in later chapters) can be helpful to identify the sequence boundaries and sedimentary 3D characteristics. Using the cross theory, we conduct the high-resolution stratigraphic framework based on electrolog, seismic, and core data. After that, we use Geoscope software importing the stratigraphic framework data and make around 600 typical instantaneous amplitude stratal slices. Compared to RMS, thickness of sand/stratal layer, and thickness of sand, the typical slices can be approximately presented the horizontal characteristics of the middle-term sequence cycle sediments. Lastly, combining vertical and horizontal boundaries of sediment deposit, we can build up a quantitative 3-D model for leading a conclusion about the study area.

## Geological background

The Dongying Depression is a complicated NE-strike extensional tectonic-unit. To the south, it includes border normal faults, northern faulted margin, Lijin Sag, Minfeng Sag, Niuzhuang Sag, central uplift belt, southern hinged margin (Ren et al. 2002; Lin et al. 2003). The Paleogene syn-rift stage consists of four main rifting episodes: (i) early initial rifting stage between the Paleogene and early Eocene (65–50.4 Ma); (ii) late initial rifting in the Middle Eocene (50.4–42.5 Ma); (iii) rift climax in the Late Eocene (42.5–38 Ma); and (iv) post rifting during the Oligocene (38–24.6 Ma) (Fig. 2).

The Paleogene strata in the Dongying Depression can be divided into three formations, namely Kongdian Formation ( $E_{1-2k}$ ), Shahejie Formation ( $E_{2-3s}$ ), and Dongying Formation ( $E_{3d}$ ), respectively (Feng et al. 1990). The lower part of second member of the Kongdian Formation consists of conglomerate and sandstone, while the upper part of second

member of the Kongdian Formation is composed of gray mudstone, oil shale, and salt layer (Xie et al. 2001). The first member of the Kongdian Formation consists of sandstone and mudstone (Feng et al. 1990). Furthermore, the fourth member of the Shahejie Formation consists of sandstone and mudstone interbedded with saline deposits (Feng et al. 2013). Moreover, the third member of the Shahejie Formation consists of dark mudstone, oil shale, and sandstone (Wang 2005). And the lower strata of the second member of the Shahejie Formation consist of conglomerates, sandy gravels, and sandstone interbedded with gray-to-red mudstone (Zhu et al. 2011a, b). The upper strata of the second member of the Shahejie Formation consist of conglomerates, coarse sandstone, fine sandstone interbedded with gray-to-red mudstone (Lin et al. 2003). The first member of the Shahejie Formation consists of fine sandstone, gray-to-red mudstone, and shale interbedded within limestone (Lin et al. 2003). Lastly, the Dongying Formation consists of coarse-to-fine sandstone and gray mudstone (Ren et al. 2002). As for the thicknesses of different formations, the thickness of Kongdian Formation is the greatest, about 500–2000 m, and the first member of Shahejie Formation is the thinnest, about 50–40 m (Feng et al. 2013). The thickness of the second member of Shahejie Formation is about 100–600 m, 300–1200 m for the third member, and 200–1000 m for the fourth Member (Feng et al. 2013). The different thicknesses of these formations may be mainly controlled by the structure evolution (Feng 1999). For example, during the deposition of the Kongdian Formation, because of the rifting episode 1 and long-term subsidence, the thickness of the formation is up to 2000 m, whereas the thickness of the third member of the Shahejie Formation is up to 1400 m resulting from the dramatically increasing strength of rifting episode 3 (Feng 1999).

The depositional systems in Dongying Depression can be classified into six facies: fan delta, braided delta, fluvial delta, sub-lacustrine fan, shallow-lake, and deep-lake deposits (Wang 2005). The architecture of sequence and sediment in the different tectonic-belts of the depression is complicated because of the A/S (accommodation space/sediment supply) which is mostly influenced by the tectonic movement rate. For example, at fault margins,  $A/S < 1$ , fan delta is the main facies, and at hinged edge with  $A/S = 1$ , the incised channel, sub-lacustrine fans, braided delta, and fluvial delta are dominating. At the axis of basin with  $A/S > 1$ , the shallow-lake is an important element (Zhu et al. 2011a, b).

## Well-based analysis of sedimentary facies

The fluvial delta deposit system is characterized on seismic reflection profile as typical sigmoidal clinoforms produced by several progradation of delta lobes (Zhu et al. 2011a, b). They can also be recognized in electrolog as upward-coarsening and

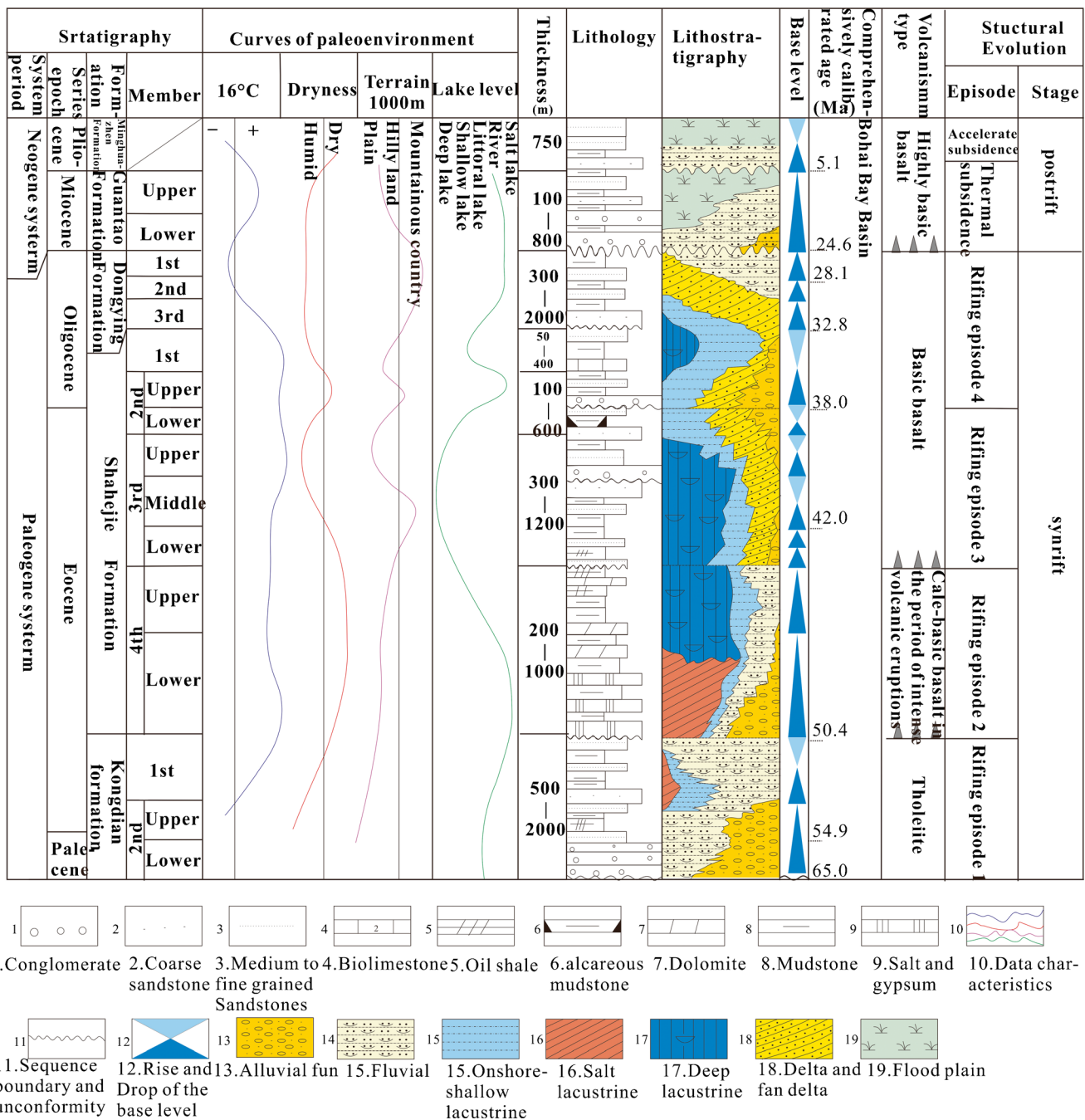


**Fig. 2** The general sequence stratigraphic charts of the Dongying Depression. During the second member of the Shahejie Formation, the weather is warm with humid-to-dry dryness and a fall-to-rise lake level (after Feng et al. 2013)

thickening successions capped by cylindrical or bell-shaped patterns (Dong et al. 2015). Furthermore, the sedimentary deposit records thick-bedded sandstone, mudstone and silt in upward-fining intervals with cross-bedding, and bell- or funnel-shaped log curve (Zhu et al. 2011a, b). Specifically, meandering river delta has been widely developed due to the development of mouth bar and fine sediments in channels within delta plain, such as mudstone and siltstone contrasting with coarse-grained fan delta (Reading and Collinson 1996).

Moreover, the upward-coarsening well-log patterns are characterized as delta front. Cylindrical or bell-shaped patterns are identified as delta plain (Dong et al. 2014).

Grain size analysis is a method to determine the size and percentage of sediment or detrital particles (Zhen et al. 2012). Grain size related to sedimentary environment is a function of hydrodynamics, which is controlled by water energy (Flemming 2007). Therefore, grain size analysis has been an efficient way to determine sedimentary transports and analyze

the sedimentary environment (Zhou and Cao 2010). As for this paper, the samples of X16, X49, and X98 were collected and then used to analyze the sedimentary transports and environment, which will be interpreted later.

### Delta plain subfacies

Meandering river delta plain is basically divided into two microfacies, based on the core and well-log data analysis, which are distributary channel and inter-channel respectively. Their characteristics are demonstrated as follows: (i) distributary channel mainly consists of siltstone and fine-to-medium sandstone, associated thick wedge cross-bedding, upward-fining intervals, and bell-shaped SP curve. The thickness of single channel is about 2–4 m. At 2247–2249 m in the Well X16, the probability cumulative curve of distributary channel is at medium-to-high amplitude in two-section form and its minutiae are about 2 . The graph indicates that the saltation component is around 95% of all sedimentary transports, with about 5% suspension component. Furthermore, the C-M graph shows that all samples are concentrated on PQ and QR sections. The biggest grain size is about 0.15–0.55 mm, indicating that the sediment of distributary channel is fine size with great sorting, mainly controlled by saltation and suspension transports; and (ii) inter-channel microfacies mainly consists of dark-to-red mudstone and shale, associated horizontal bedding and straight SP curve (Fig. 3). The thickness of single inter-channel is about 3–6 m. Generally, delta plain has developed the interbedded sandstone and gray-to-black mudstone, with cross-bedding and upward-fining intervals. The thickness of delta plain is about 300 m.

### Delta front subfacies

Meandering river delta front is divided into three microfacies, namely mouth bar, underwater distributary channel, and tributary bay. Their characteristics are demonstrated as follows: (i) mouth bar mainly developed in MSC6 and MSC7, with fine-medium sandstone associated thick wedge cross-bedding, upward-coarsening intervals, and funnel-shaped SP curve. The thickness of single mouth bar is about 3–5 m. For interval of 2549–2552 m in the Well X98, the probability cumulative curve of mouth bar is at medium amplitude in three-section form, and its minutiae are about 2 . This graph indicates that the saltation component is around 87% of all sedimentary transports, with about 15% suspension component. Furthermore, the C-M graph shows that all samples are concentrated on PQ and QR parts. The biggest grain size is about 0.05–0.35 mm, indicating that the sediment of mouth bar is fine with great sorting, mainly controlled by saltation and suspension transports; (ii) underwater distributary channel consists of fine-to-medium sandstone associated thick wedge cross-bedding, upward-fining intervals, and bell-shaped SP curve (Fig. 4). The thickness of single underwater distributary channel is around 2–4 m. For interval of 2449–2451 m in the Well X49, the probability cumulative curve of underwater distributary channel is at medium-to-high amplitude in two-section form, and its minutiae are about 2 . This graph indicates that the saltation component is around 75% of all sedimentary transports, with about 25% suspension component. Furthermore, distributary channel in delta plain and the underwater distributary channels are similar in deposit; and (iii) tributary bay is usually the dark mudstone, associated horizontal bedding and straight SP curve (Fig. 5). Generally, the delta front developed upward-fining intervals of medium-to-fine

**Fig. 3** Interpretation for the channel and inter-channel microfacies based on wire-line-log facies and core facies. The channel is bell-shaped in SP and its C-M graph shows the short NO, PQ, QR, and RS segment. The short NO segment indicates the normal rolling movement with a few gravel. The OP, PQ, and QR segment shows the suspension movement within little rolling way. The short RS segment indicates the less homogeneous suspension movement, which reflects the characteristics of distributary channel in delta plain (Well X16)

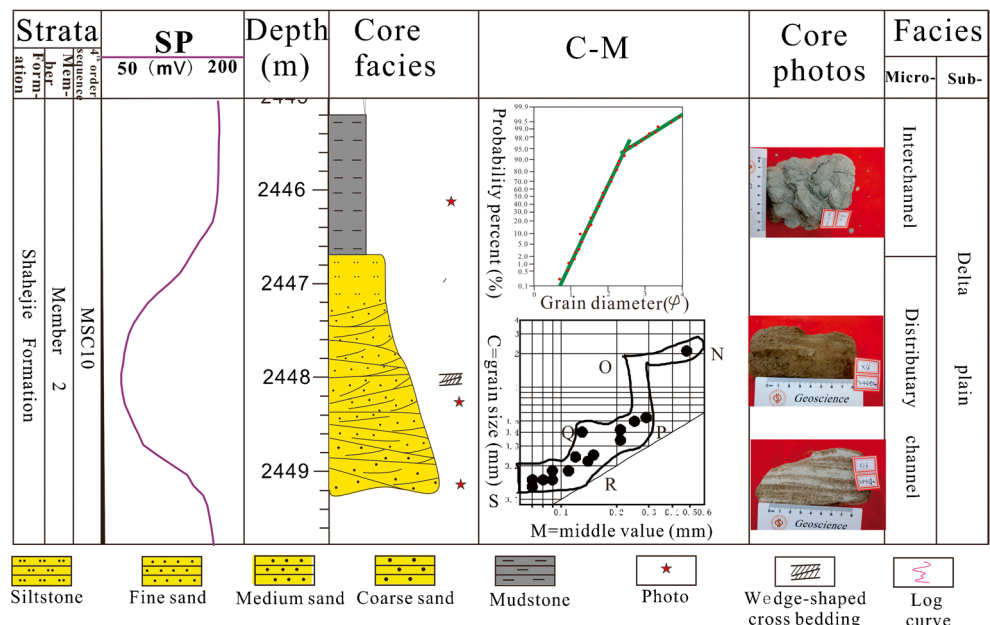
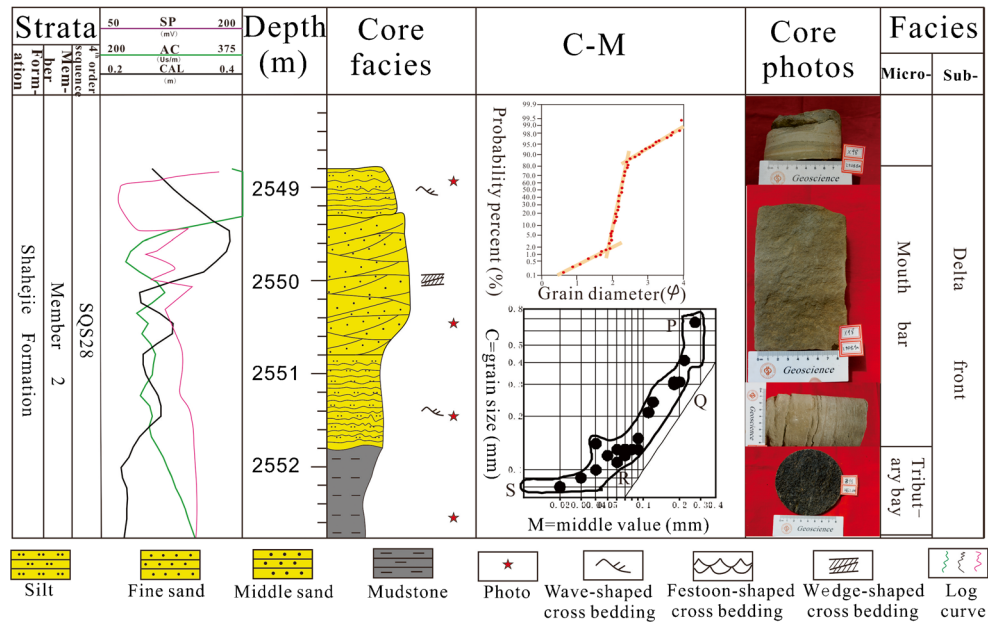


**Fig. 4** Interpretation for the mouth bar and tributary bay microfacies based on wire-line-log facies and core facies. The mouth bar is funnel-shaped in log curve and its C-M graph shows the PQ, QR, and RS segment. The segment indicates the dominating homogeneous and gradually changed suspension movement with a little rolling way, which reflects the characteristics of mouth bar in delta front. And the tributary bay developed mudstone with carbon fragment (Well X98)



sandstone in underwater distributary channels, and upward-coarsening interval of fine-to-medium sandstone in mouth bar. The thickness of delta front is around 300 m.

Figure 6 directly shows the characteristics of different microfacies in response to core facies and electricity based on the data of study area. Significantly, the distributary channel presents the sandstone with upward-fining interval, whereas the mouth bar indicates the upward-coarsening interval. As for SP curve, the channel is bell-shaped, while the mouth bar is funnel-shaped. Furthermore, the probability cumulative curve of distributary channel is at medium-to-high amplitude in two-section form, and its minutiae are about 2. But there are differences between under water distributary channel in

delta front and distributary channel in delta plain. For example, the percentage of saltation is about 95% in distributary channel, while it is around 75% in underwater distributary channel. To the lacus, the saltation's percentage is decreasing and it indicates the decreasing energy of water dynamic. Specially, the probability cumulative curve of mouth bar is at medium-to-high amplitude in three-section form (Fig. 6).

### Sequence stratigraphic framework

After the 1980s, sequence stratigraphy classification has developed into three main bands, namely Vial's classic, Galloway's

**Fig. 5** Interpretation for underwater distributary channel and tributary bay microfacies based on wire-line-log facies and core facies. The underwater distributary channel is bell-shaped in log curve, and the grain size probability graph of channel indicates that it consists of two members, with around 75% as the critical point between suspension and saltation component. The tributary bay is pure mudstone (Well X49)

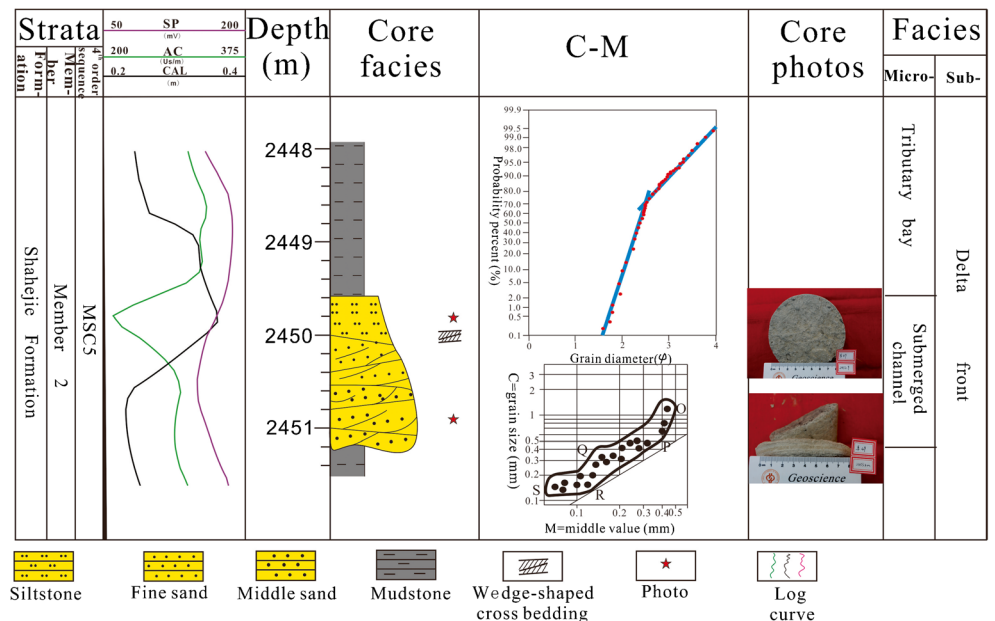
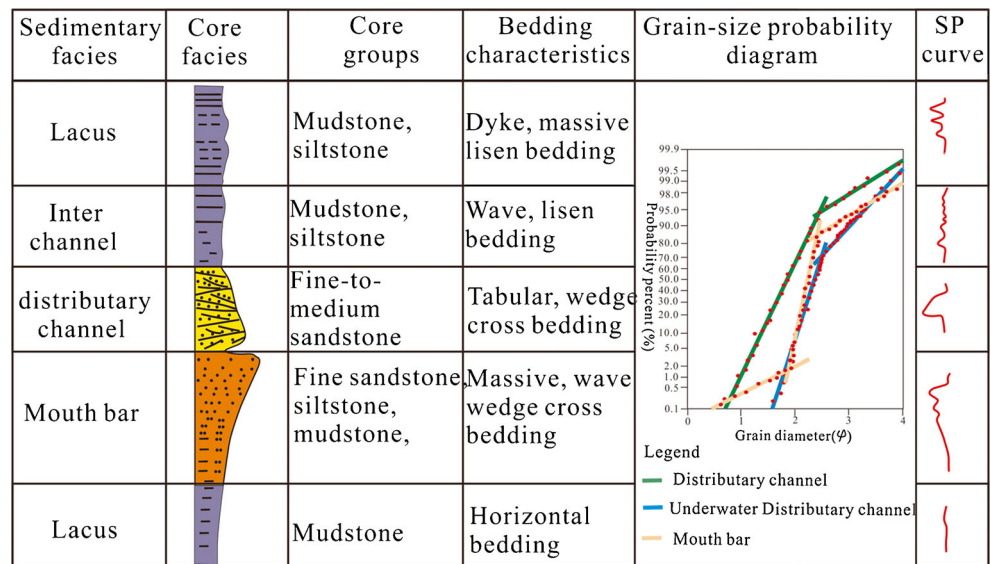


**Fig. 6** The schematic diagram of core facies in relation to electricity. The channel is upward-fining interval with bell-shaped in SP log curve, while mouth bar is upward-coarsening interval with funnel-shaped in SP log curve



genetic, and Cross high-resolution sequence stratigraphy (Vail et al. 1997; Cross 1988; Galloway 1989; Catuneanu et al. 2009). As for this project, it is based on cross high-resolution theory.

Generally, high-resolution stratigraphic base-level cycle is used to identify stratigraphic framework within the third sequences. It is an important step to identify different base-level cycle orders and boundaries, based on the change of accommodation space/sediment supply (A/S), sedimentary foundation, and so on. Table 1 shows the detailed principles (Zhu et al. 2011a, b).

This study moves forward to demonstrating a high framework upon the following methods (Wu et al. 2000; Xie et al. 2001; Wang 2005; Zhu et al. 2011a, b). Firstly, we have identified the short-term sequence cycle (SSC) according to change of lithology and log. Secondly, the middle-term sequence cycle (MSC) is made by different

patterns of SSC. Thirdly, we have identified the seismic termination for the long-term sequence cycle (LSC) boundary. Finally, the high-resolution stratigraphy of the second member of the Shahejie Formation in the study area is classified into several 40–45 SSCs, 14 MSCs, and 2 LSCs (Fig. 7).

**Short-term sequence cycle characteristic**

The boundary of short-term sequence cycle is the fifth sequence, with a duration of 0.1–0.5 Ma and deposit thickness of 8–12 m. The borehole in study area developed about 45 SSCs (namely SSC1–SSC45 from bottom-up) that can be classified into three types (asymmetric base-level fall cycle, asymmetric base-level rise cycle, and symmetric base-level cycle) with seven sub-types.

**Table 1** The characteristics of high-resolution sequence stratigraphy of the Shahejie Formation (after Zhu et al. 2011a, b)

Order	Boundary genetic types	Identification principle	Main controls	Vail theory	Cross theory
II	Unconformity or relative boundary related to stress field change during different tectonic evolution	Tectonic-scale unconformity in outcrop; incised erosion surface; log dramatic change; seismic main reflection	Stress field change during different tectonic evolution	Sequence set	Super-long-term base-level cycle
III	Unconformity or relative boundary related to the change of tectonic episode strength and sedimentary foundation during the same tectonic stress field	Large-scale unconformity in outcrop; incised erosion surface; log dramatic change; seismic termination	The change of tectonic episode strength	Sequence	Long-term base-level cycle
IV	Relative conformity or sedimentary discontinuous boundary related to climate and sediment supply	Resident sediment and erosion surface in core; log patterns' change	Astronomic eccentricity period	Para-sequence set (or systems tract)	Middle-term base-level cycle
V	Local erosion surface or relative conformity related to A/S	Resident sediment and erosion surface in core; log change; lithological drama change	Astronomic obliquity period	Para-sequence	Short-term base-level cycle

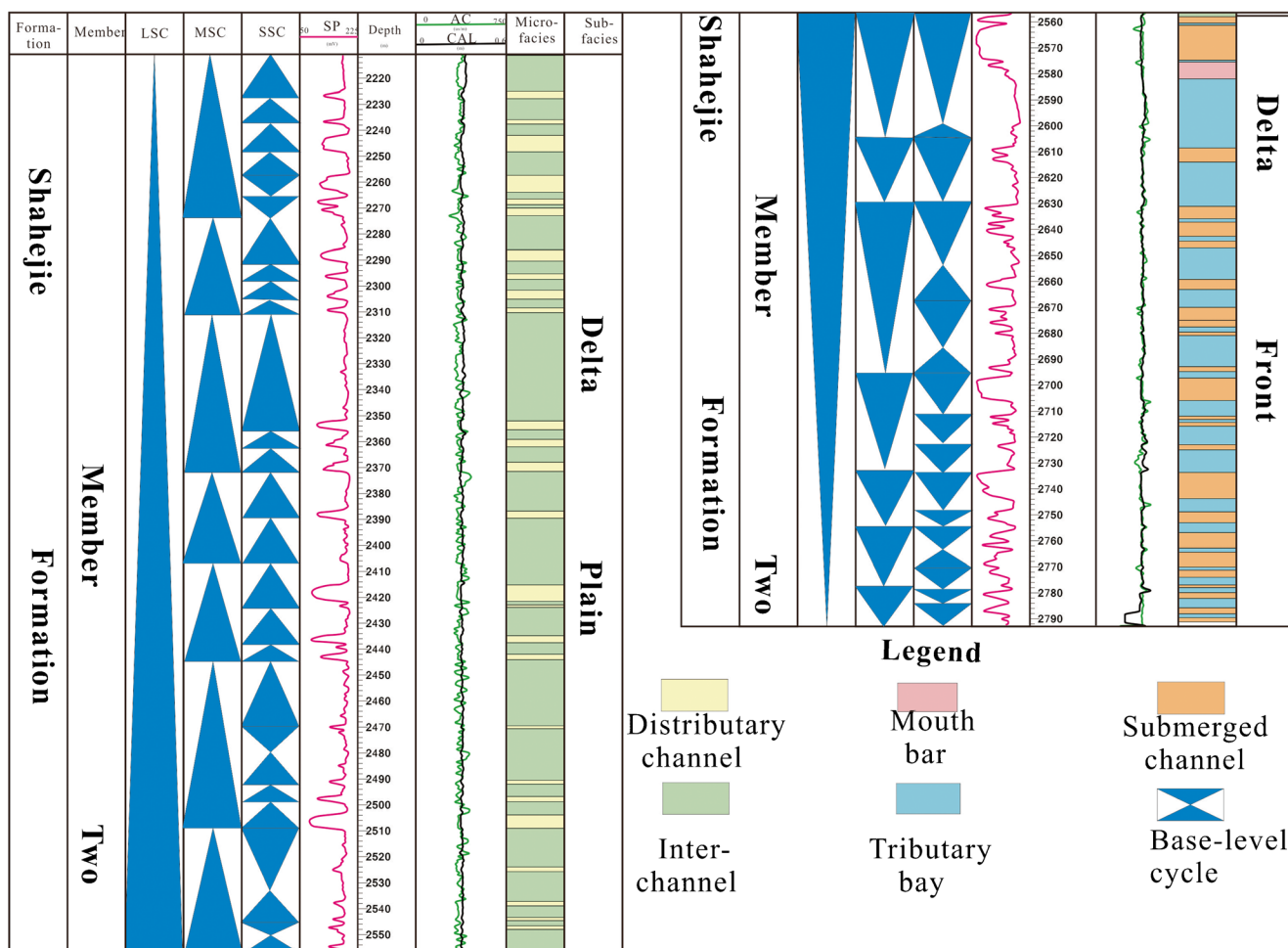


**Fig. 7** Typical stratigraphic log indicates the characteristics of the second member of the Shahejie Formation in the Dongying Depression, alongside the spontaneous potential (SP), acoustic log (AC), and caliper (CAL). Data of wire-line-logs is originated from Well X37–34

### Asymmetric base-level rise cycle

The tendencies of cycle symmetries change as a function of shifts in the accommodation space/sediment supply ratio. The upper part of the second member of the Shahejie Formation mainly developed asymmetric base-level rise cycles during delta plain deposit stage. Its characteristics are as follows: (i) the delta plain develops base-level rise cycles; (ii) the bottom of base-level cycle is erosion surface with bell-shaped or box-shaped log curve; and (iii) the location of the study area is near the sediment source or abundant sediment supply.

According to the change in accommodation space-sediment supply ratio, we could classify the asymmetric base-level rise cycle into two sub-types, namely low accommodation (A1) and high accommodation (A2). A1 mainly developed, at upstream position of delta plain, coarse-to-medium sandstone, erosion surface, upward-fining intervals, and its lack of mudstone; whereas, A2 mainly developed, at middle-to-downstream delta front, fine-to-silt sandstone, upward-fining intervals, and its lack of underwater distributary channel erosion (Fig. 8A).

### Asymmetric base-level fall cycle

Its characteristics are as follows: (i) the delta front develops base-level fall cycle; (ii) the top of base-level cycle is discontinuous surface with funnel-shaped or box-shaped log curve; and (iii) the location of the study area is far away from the sediment source but generally abundant sediment supply.

According to the change in accommodation space/sediment supply ratio, we could classify the asymmetric base-level fall cycle into two sub-types, namely low accommodation (B1) and high accommodation (B2). B1 mainly developed, at mouth bars and upstream position of delta front, silt-to-coarse sandstone, discontinuous surface, upward-coarsening intervals, and its lack of mudstone; whereas, B2 mainly developed, at middle delta front, silt-to-fine sandstone with upward-coarsening intervals, the bottom with lithology turn-around surface (Fig. 8B).

### Symmetric base-level cycle

In this study area, the characteristics of symmetric cycle are as follows: (i) the boundary between base-level rise cycle and



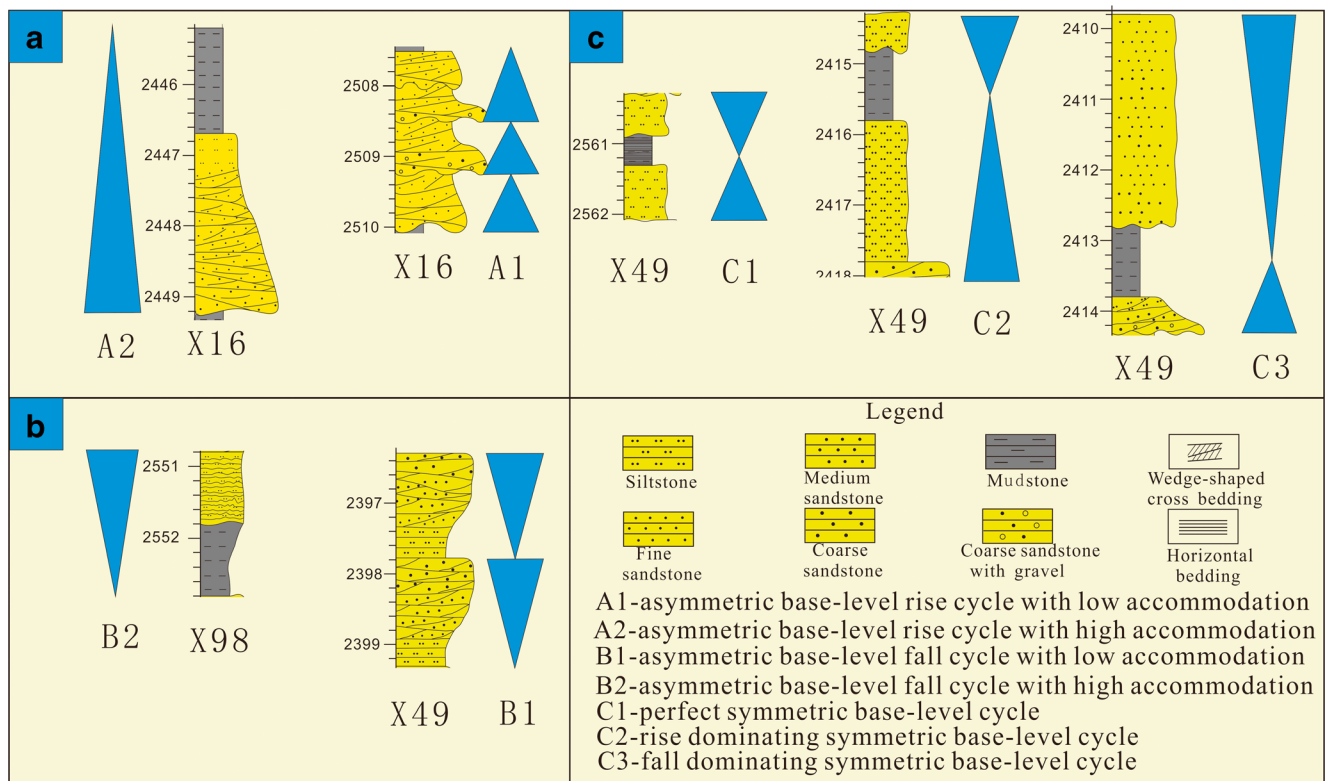


**Fig. 8** The characteristics of different cycle structures in the study area during the second member of the Shahejie Formation. The cycle can reflect the condition of sediment supply or the location of the well in

sedimentary systems. For example, A1 may indicate the abundant sediment supply or the location near the sediment source

base-level fall cycle is a flooding surface; (ii) upward-coarsening with a funnel-shaped log curve pattern and upward-fining intervals with bell-shaped log curve pattern; (iii) accommodation space/sediment supply ratio is about 1; and (iv) it is classified into three sub-types, namely perfect symmetric base-level cycle (C1), rise dominating symmetric cycle (C2), and fall dominating symmetric cycle (C3) (Fig. 8C).

The characteristics of short-term base-level cycle of the second member of Shahejie Formation in the study area are as follows: (i) it develops delta plain and front with asymmetric cycles and symmetric cycles types; (ii) the base-level rise cycle is dominating in delta plain during the upper part of the second member of Shahejie Formation, whereas the base-level fall cycle is dominating in delta front during the lower part; (iii) different short-term cycle structures indicate deposit record change, and coarse sediment developed around the fall-to-rise turn-around which means the lower part of the base-level rise cycle and upper part of the base-level fall cycle.

**Middle-term sequence cycle characteristic**

Middle-term sequence cycle is bounded by the fourth sequences, with a duration of 0.5–1.0 Ma and deposit thickness of 20–100 m. Normally, MSCs are symmetric cycles with base-level rise and fall cycle. Vertically, MSCs consist of

several similar SSCs. The Shahejie Formation in the study area consists of 14 MSCs (namely MSC1–MSC14 from bottom-up) and every MSC consists of 2–4 SSCs. Furthermore, the cycle structure of MSC is divided into two types, namely asymmetric base-level rise cycle and base-level fall cycle.

The characteristics of MSCs are as follows: (i) the asymmetric base-level rise cycles develop at delta plain, (ii) the asymmetric base-level fall cycles develop at delta front, and (iii) the coarse sediment is dominating in the channel at lower base-level rise cycles and mouth bar at upper base-level fall cycles.

**Long-term sequence cycle characteristic**

Long-term sequence cycle is bounded by the third sequences, with a duration of 1.0–5.0 Ma and deposit thickness of 100–300 m. Normally, LSCs are symmetric cycles with base-level rise and fall cycle. Vertically, LSCs consist of several similar MSCs which develop during the same sedimentary environment. The Shahejie Formation in the study area consists of two LSCs (namely LSC1–LSC2 from bottom-up) and every LSC consists of seven MSCs. Furthermore, the cycle structure of LSC is divided into two types: symmetric base-level rise cycle and base-level fall cycle.

During the LSC deposit stage, several MSCs’ genetic patterns lead to three different pattern styles, namely aggradation,

retrogradation, and progradation. As for the detail, aggradation mainly develops during the middle stage of base-level rise cycle or the early stage of base-level fall cycle, with  $A/S = 1$ . Retrogradation mainly develops during the medium-to-late stage of the base-level rise cycle, with  $A/S > 1$ . Progradation mainly develops during the late stage of the base-level rise cycle, with  $A/S < 1$ .

The characteristics of LSC are as follows: (i) the base-level rise cycle develops at delta plain; (ii) the base-level fall cycle develops at delta front; (iii) the trend of fall-to-rise turn-around in LSC is similar to that in MSC; and (iv) the thickness of base-level rise and fall cycle is similar.

### High-resolution sequence stratigraphic framework

Multiple orders of base-level cycles are fundamental for the high-resolution sequence stratigraphic framework. Using isochronous stratigraphic correlation principle (sequence boundaries and flooding surfaces), the framework of the second member of the Shahejie Formation shows several indications (Fig. 9).

The sediment source of the study area in the second member of the Shahejie Formation is mainly in EW direction (Feng et al. 2013). Based on that, we have analyzed the base-level cycle relation during delta deposit stage.

- (1) The delta front develops during MSC1–MSC7, whereas the delta plain develops during MSC8–MSC14. Erosion surface is the fall-to-rise turn-around.

- (2) Channel in delta plain, underwater distributary channel, and mouth bar in delta front mainly develop around the fall-to-rise turn-around. The mouth bar mainly develops during the MSC6–MSC7. As for the SSC, it mainly consists of the asymmetric base-level rise and fall cycles.
- (3) The retrogradation is the dominating pattern during the LSC2, whereas the progradation is the dominating pattern during the LSC1. As for the detail, the lithology in LSC1 is generally coarser than that in the LSC2.

### Study of seismic geomorphology

The study of seismic geomorphology includes the following steps (Zhu et al. 2011a, b; Dong et al. 2015). Firstly, it is crucial to make sure about the correction of sequence stratigraphic framework. Secondly, the stratal volume is made for this study area by flattening the reference horizons in the second member of the Shahejie Formation. Thirdly, based on Geoscope software, 4525 instantaneous amplitude stratal slices, almost covering the whole 400-ms seismic data intervals, are made for interpretation between top sequence boundary and bottom sequence boundary. After that, the most important work is to make an interpretation for the sedimentary systems based on the typical instantaneous amplitude stratal slices and well data analysis (Zeng et al. 1998).

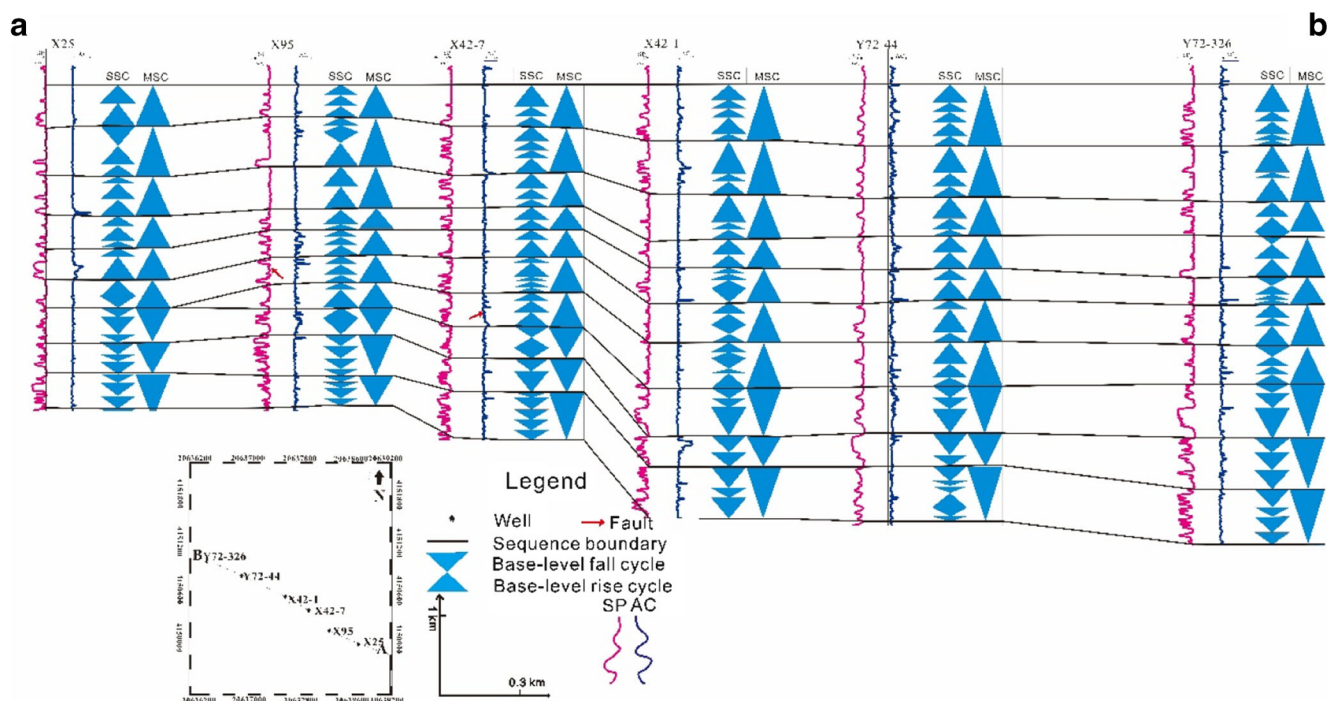


**Fig. 9** Stratigraphic cross-section A–B showing middle-term sequence cycles (MSCs) and short-term sequence cycles (SSCs) within the Shahejie Formation. The AB cross-section consists of X25, X95, X42-7, X42-1, Y72-44, Y72-326. The base-level rise cycles mostly develop in the upper part

### Relationship between attribute and lithology

There are two ways to combine the seismic attribute with lithology. On the one hand, the acoustic impedance (AI) is great to make a relationship between seismic attribute and lithology. It basically uses the synthetic seismogram as a bridge to connect AI with lithology for distinguishing sandstone and mudstone in vertical profile (Fig. 10A and B). Secondly, based on the same well coordinate system, the well-log data curves is compared with instantaneous amplitude stratal slices to calculate the seismic attribute with log facies in horizontal profiles (Fig. 10C). As a

result, it apparently indicates that the sandstone, in response to bell-shaped or funnel-shaped curve in well data, is white color (negative attribute) in the study area, whereas the black color (positive attribute) mainly indicates the mudstone.

### Interpretation of stratal slices

Although researches have been conducted on Dongying Depression, it is still unclear about the microfacies distribution in the study area (Wu et al. 2000; Xie et al. 2001; Wang 2005; Zhu et al. 2011a, b). Based on the high-resolution sequence

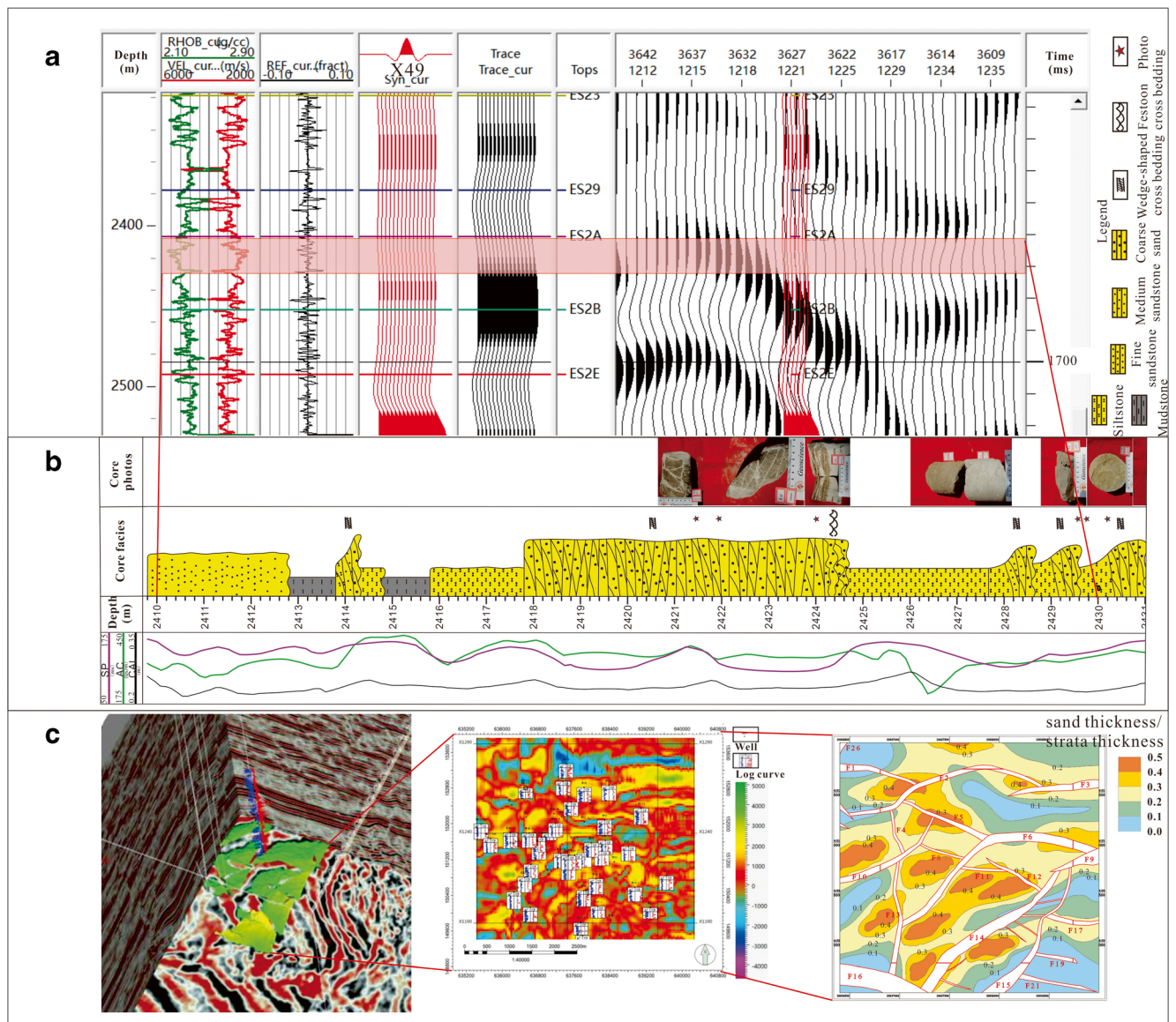


**Fig. 10** Using the well-derived calculated synthetic seismogram can establish well-to-seismic correlation in the stratal slice. A: the synthetic seismogram connecting log data to seismic data. B: the sandstone in response to positive amplitude in seismic data and log curves. C: the left showing the seismic volume in response to log curves; the middle presenting the typical instantaneous amplitude slice. Compared to the log

data, the strongly positive amplitude (red color) mostly denotes thick sandstone, whereas the negative amplitude (blue color) is predominately tied to shale beds; the right graph: the sand thickness/strata thickness indicating the high value in graph in response to sandstone. The combination of typical slice and sand thickness/strata thickness can interpret the distribution of microfacies

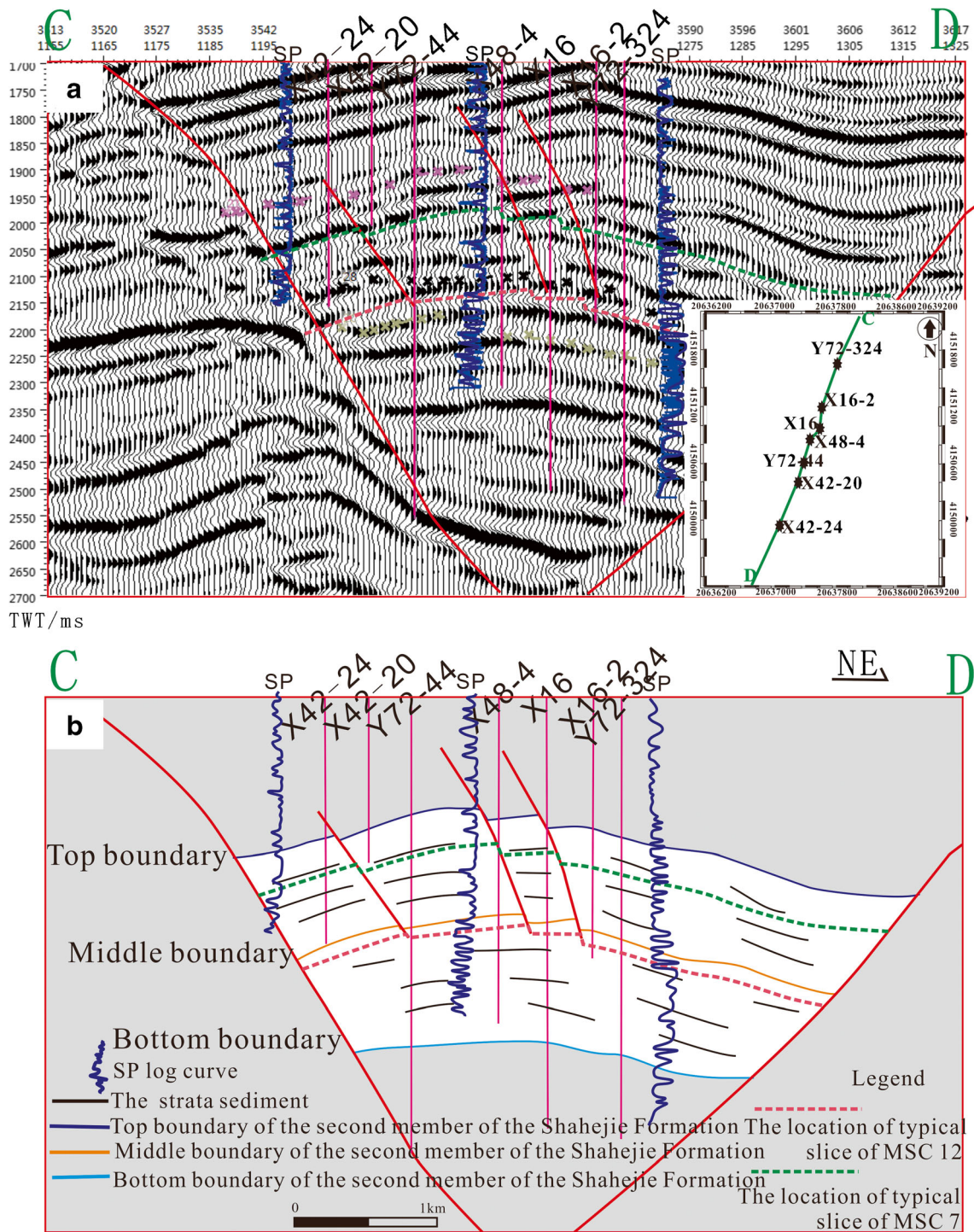


**Fig. 11** Uninterpreted seismic cross-section (A) and interpreted seismic cross-section (B). These photos show the location of typical stratal slice during MSC12 and MSC7 deposit stage. There is a lack of several MSC

between MSC1–7, and the A graph indicates the different log curve pattern between MSC1–7 and MSC8–14, which reflects that the A/S in the delta plain is bigger than that in the delta front

framework, the specific location of these typical stratal slices is shown in Fig. 11. Figure 12A' and B' shows pictures of these typical instantaneous amplitude slices, which indicate the distinguished deposition characteristics in different sedimentary periods of the second member of the Shahejie

formation. Along the high-resolution sequence boundary, we have made abundant instantaneous amplitude stratal slices of MSCs, and selected similar typical instantaneous amplitude stratal slices to present the deposition characteristics of the same MSC while considering characteristics of log curves

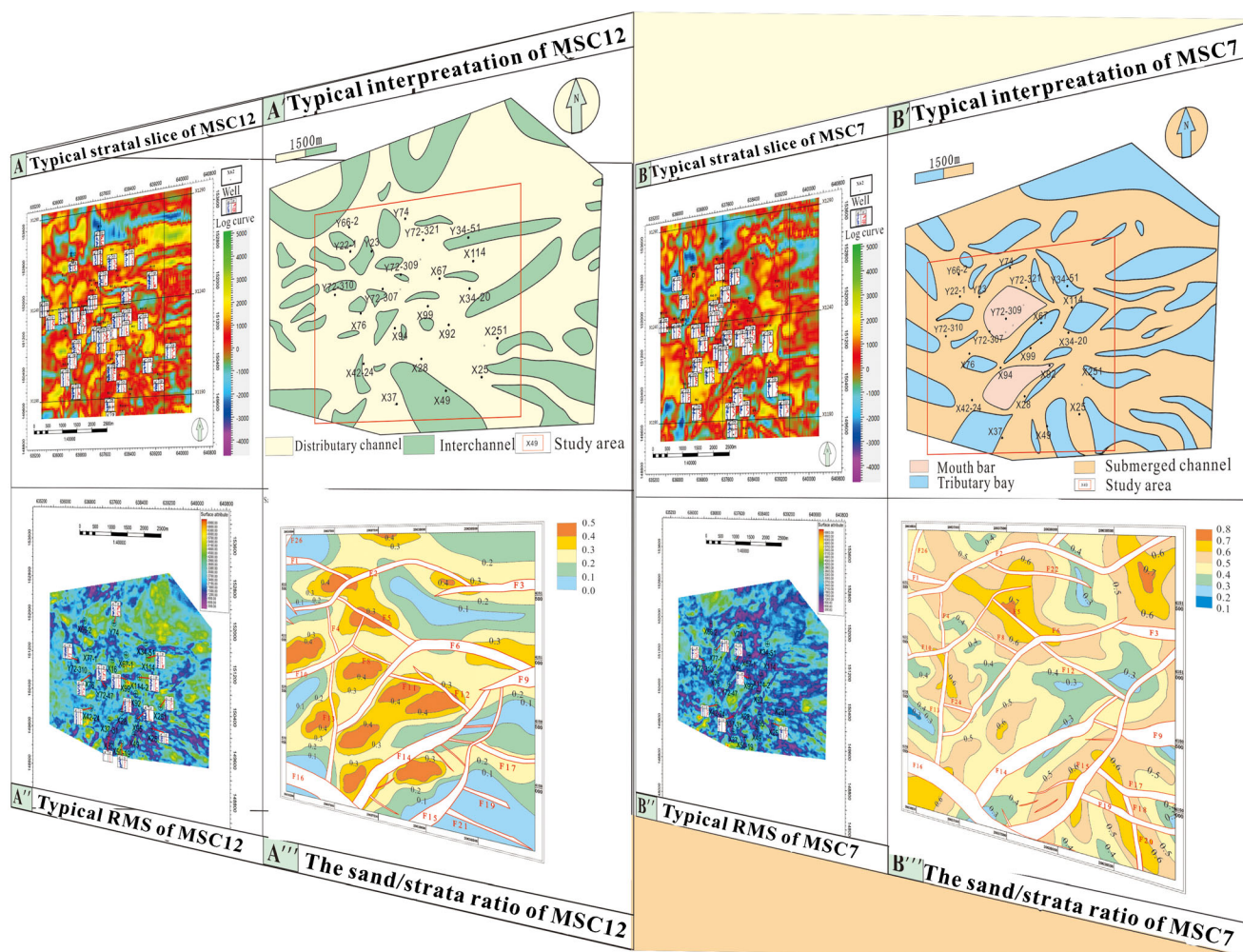


**Fig. 12** Comprehensive analysis of MSC12 and MSC7 typical stratal slices. A and B typical instantaneous amplitude stratal slices of MSC12-S155 and MSC7-S260; A' and B' interpreted sedimentary facies

distribution; A'' and B'' RMS maps in response to log curve; A''' and B''' the sand/layer ratio of different deposit stages indicating the sandbody distribution

and RMS property graphs. For example, the MSC12-S155 is the 155th stratal slice to indicate the horizontal sedimentary distribution in the delta plain for the MSC12.

In the typical seismic stratal slices, they apparently show that the positive attribute (red color) is almost in the central part of the study area with a SW or EW direction, about 5–7 km<sup>2</sup>. The negative attribute (blue-to-dark) is dispersed around the other parts. According to the preceding results, the red color mainly indicates sandstone and the dark color mainly is mudstone. Furthermore, the red color mainly indicates the channels and blue-to-dark color mainly indicates inter-channel in the meandering river delta plain. Also, in the meandering river delta front, the upward-fining intervals with red color mainly indicate underwater distributary channel, whereas the upward-coarsening with red color indicates the mouth bar.

Basically, the whole typical instantaneous amplitude stratal slice interpretation of 14 MSCs (MSC1–14) is made based on the same principle. Figure 13 apparently shows that (i) even though there is one single channel, the change of distribution

is frequent; (ii) there are several stripped- or massive-shaped inter-channel microfacies, around 0.25 km<sup>2</sup>. Significantly, the meandering river delta develops in the channel and mouth bar; (iii) the direction of channel is mainly EW, with maximum width of 2 km; and (iv) the sand thickness/layer thickness of delta front is significantly bigger than that in delta plain.

Mouth bars are present in the delta front environment, generally extending east to west and are diamond-shaped. Table 2 is made for better quantitative understanding about the mouth bar. For example, the maximum area of mouth bar is 1.52 km<sup>2</sup> in the study area's channel, with an average area of 0.5 km<sup>2</sup> during MSC7 and 0.70 km<sup>2</sup> during MSC6.

It is critically important to make a vertical sedimentary microfacies graph based on abundant well-logs analysis. Thus, we can better understand the 3D sedimentary characteristics. Figure 14 directly indicates that (i) the layer thickness of delta plain is larger than that in delta front; (ii) the sandstone thickness of delta front is apparently bigger than that in delta plain. For example, during the deposit stage of MSC8–14, the

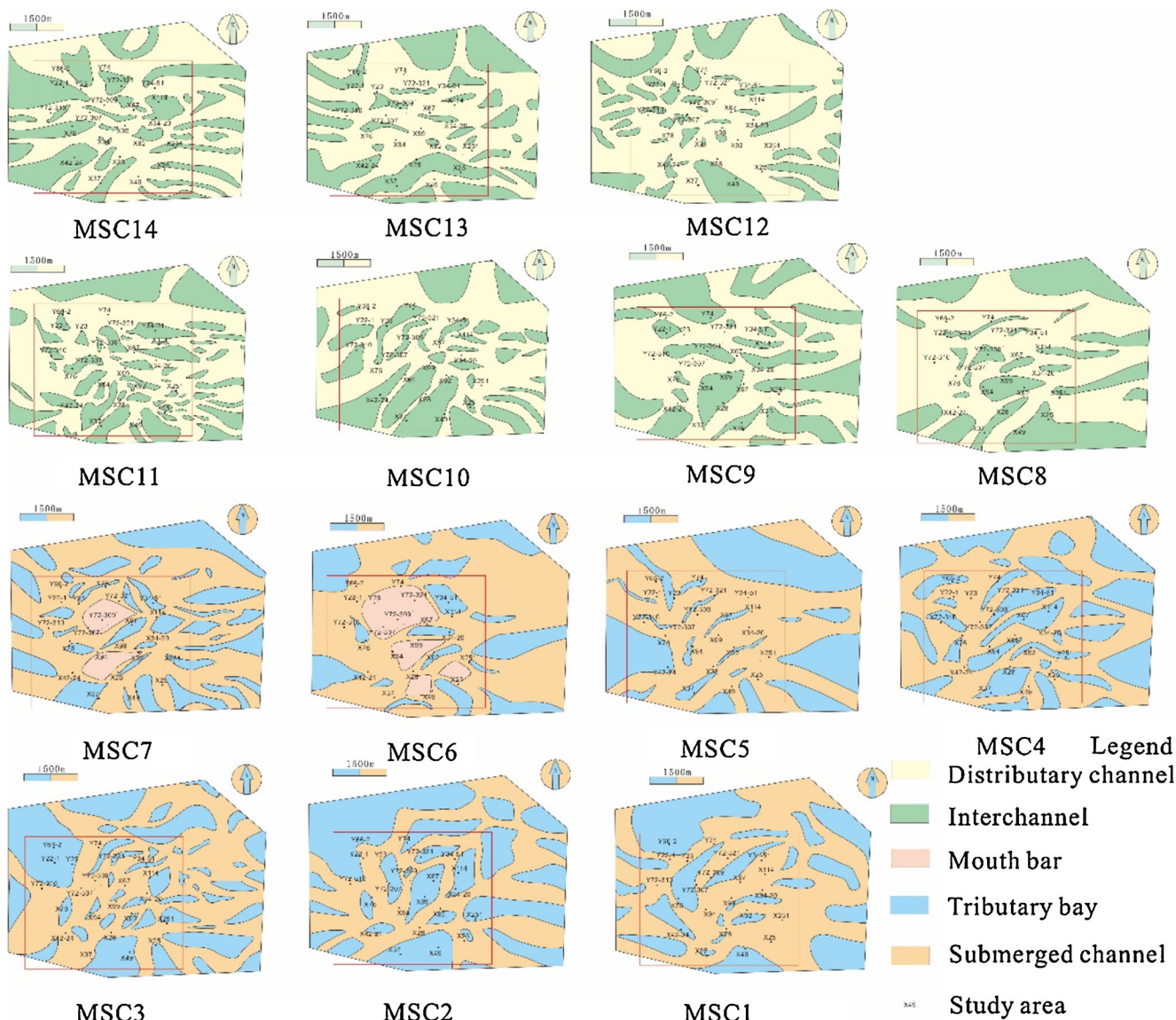


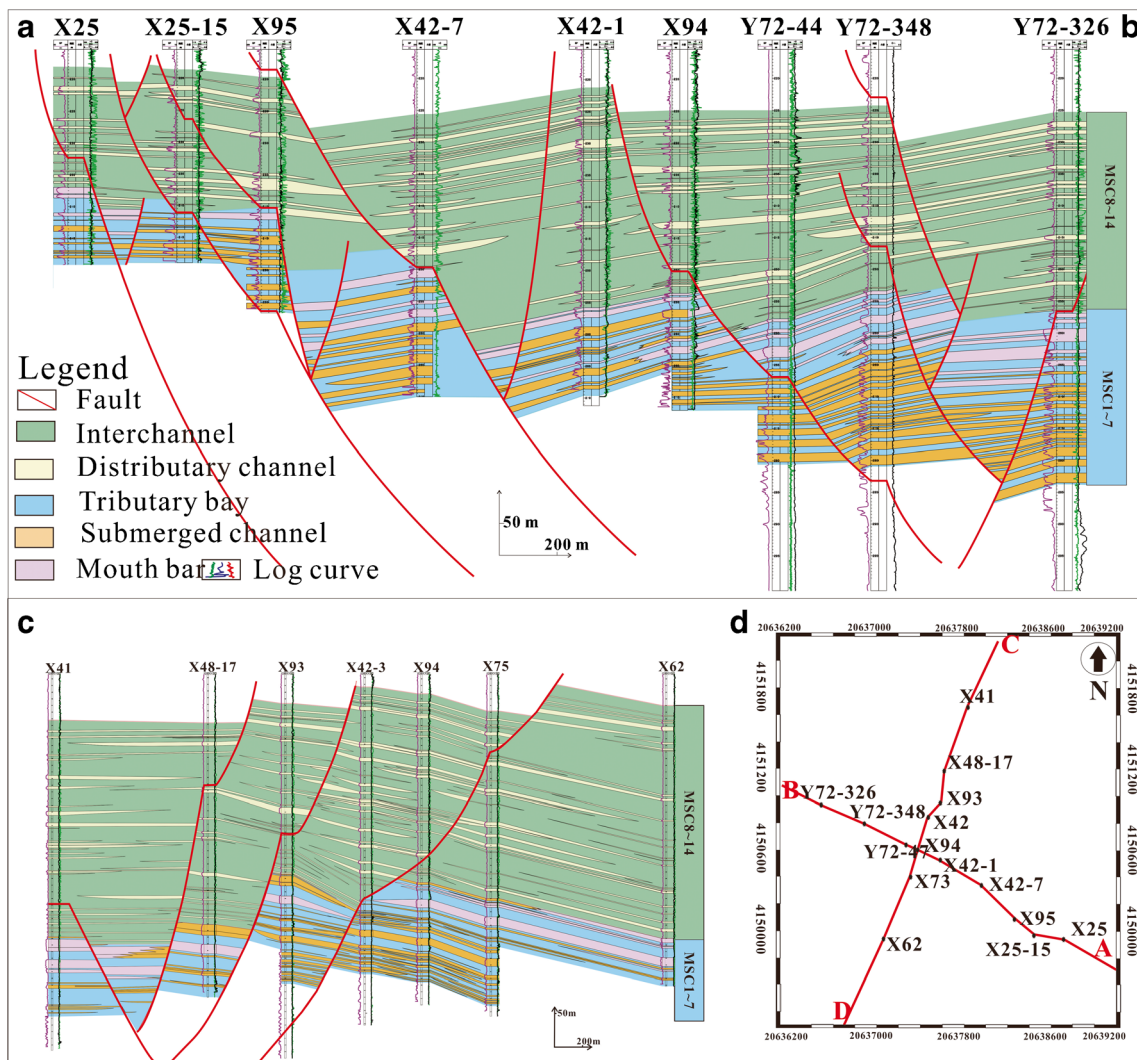
**Fig. 13** The 14 typical and interpreted stratal slices in response to 14 MSCs of the second member of the Shahejie Formation in the study area, indicating the distribution of microfacies. MSC, middle-term sequence cycle

maximum sandstone thickness is 10 m, whereas the maximum sandstone thickness during MSC1–7 is 20 m; (iii) the thickness of layer is apparently thick in the center of the study area, which has developed huge sandstone in response to the complicated channel interaction; and (iv) almost all faults in the study area are post-rift tectonic movement, which rarely affect the syn-rift stage deposits. All of these can better reflect the relationships between 3D depositional systems and sequence characteristics.

Although, Fig. 14 obviously indicates the relation between deposition and sequence characteristics of the study area; the limit of this unique direction reflection profile is inevitable. As it shows in Fig. 15, actually, the total strata thickness is similar between MSC8–14 and MSC1–7, with about 300 m for lower and upper part of the second member of the Shahejie Formation, which is significantly different from the previous result. Furthermore, the sand/strata ratio

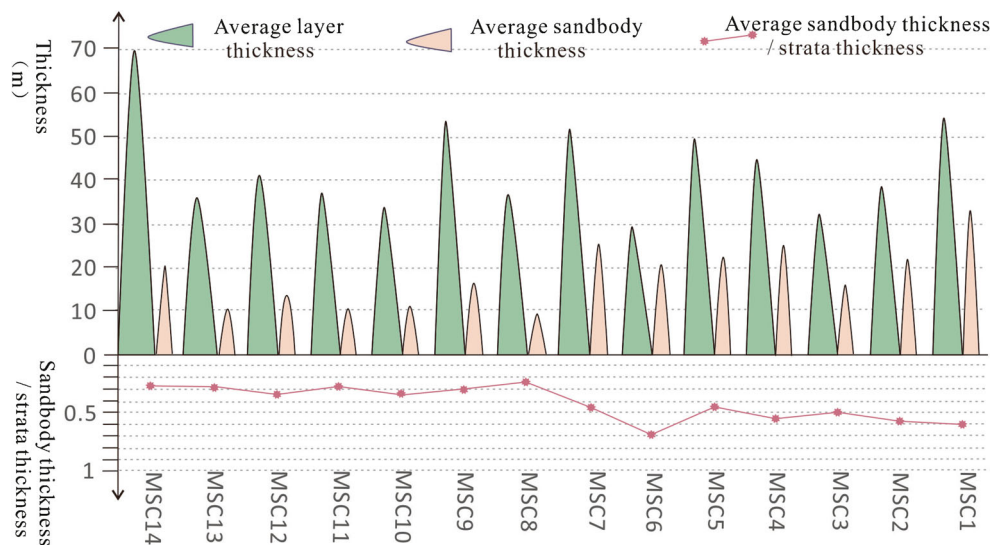
**Table 2** The area statistics of mouth bar developed in member 2 of the Shahejie Formation in the study area

Sequence	Area verified by the wells (km <sup>2</sup> )	Predicted areas (km <sup>2</sup> )
Number meaning	(Maximum area–minimum area) / average area (mouth bar number)	
MSC7	(0.86–0.22) / 0.52 (2)	(0.98–0.34) / 0.56 (3)
MSC6	(1.52–0.25) / 0.73 (4)	(1.46–0.32) / 0.68 (3)



**Fig. 14** The relation between deposition and sequence. A–B reflection indicating the characteristics along the direction of sediment supply, and C–D reflection showing the features across the orientation of sediment supply. MSC, middle-term sequence cycle

**Fig. 15** The statistic characteristics of study area. It indicates that sandbody thickness during MSC1–7 is greater than that during MSC8–14 stage



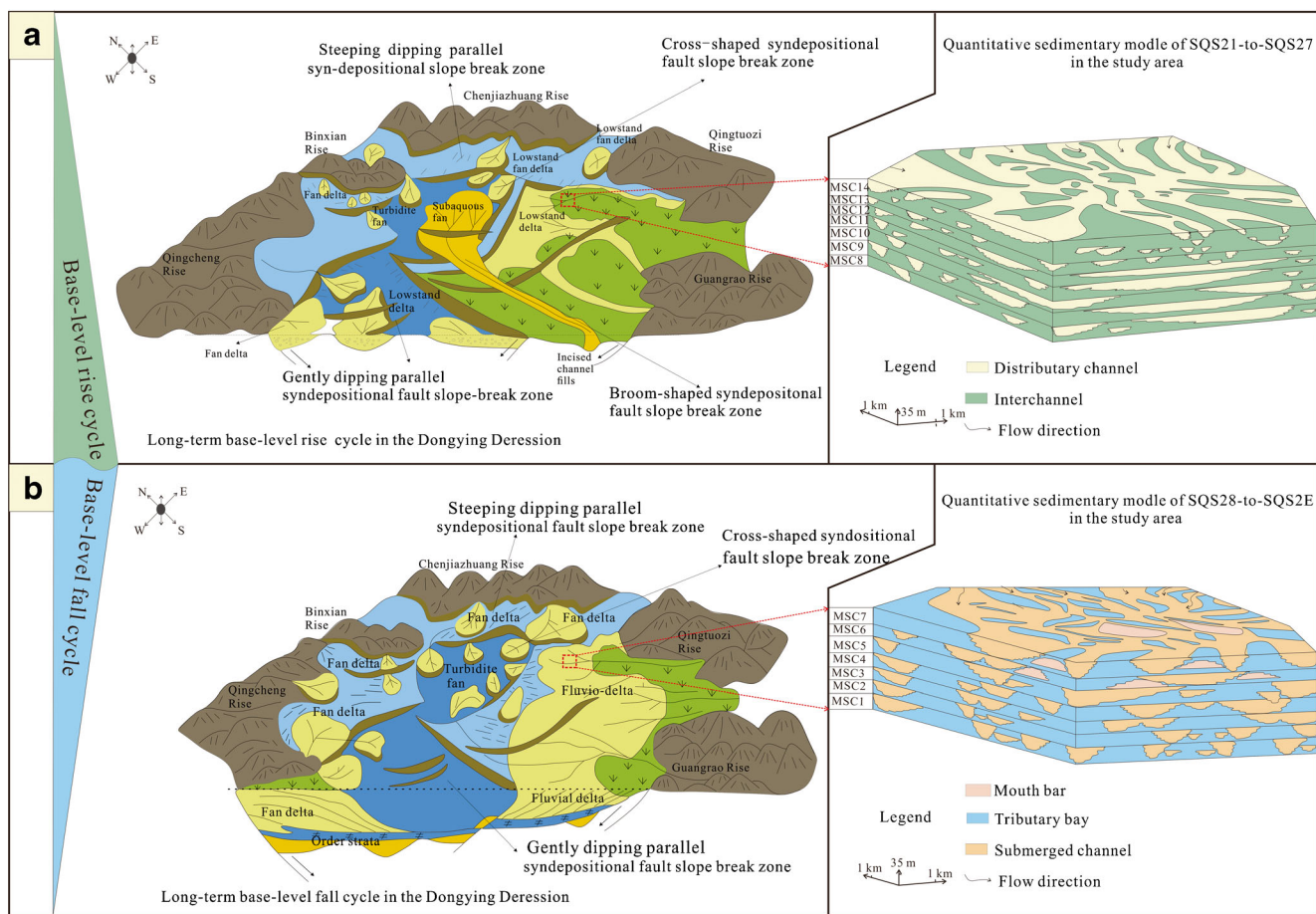


**Fig. 16** The 3D depositional evolution model of Dongying Depression (the study area is the red box) and the quantitative model of the study area indicating frequent change of channels and other microfacies during the second member of the Shahejie Formation (after Feng et al. 2013)

dramatically increases in MSC7, with around 0.3 for MSC8–14 and about 0.55 for MSC1–7, which indicates the different sedimentary environment. Thus, we take the advantage of quantitative statistic based on the information from 400 wells to produce an integrated quantitative 3D sedimentary model (Fig. 16).

## Discussion

### Delineation of sandbody based on seismic geomorphology

This study, based on the latest 3D seismic data and drilling data, innovatively puts forward a series of seismic and geomorphologic stratal slices and logging interpretation data to describe the probabilities of channel distribution in the study area. On the one hand, we show the geomorphologic characteristics of the study area. We find that even in the same river channel of the delta, the formation connecting performance is poor due to the large inter-channel area, which will challenge the oil and gas exploration and production. On the other hand,

the mouth bar is identified during the sedimentary deposition stage of MSC6–7, which are base-level fall cycle. Furthermore, we innovatively demonstrate the boundary of mouth bar during those times to quantitatively reflect the distribution of mouth bar based on the seismic geomorphology and well-logs data analysis. Even though it is a complicated block with deep burial depth, using seismic geomorphology and well-logs analysis is a great way to understand the distribution of sedimentary deposit systems in a 3D scale for further exploration.

### Depositional and evolution characteristics

Based on several previous sedimentary deposit works (Wang 2005; Feng et al. 2013), Feng et al. put forward a concept model for the second member of Shahejie Formation in Dongying Depression based on the analysis of sediment characteristics, stratigraphic sequence, tectonic-sedimentary architecture, and deposit features in large-scale (Fig. 16 left). Obviously, according to their points, long-term base-level cycle is controlled by syn-depositional fault (Feng et al. 2013). The A/S ratio is complicated because of tectonic movement



(Zhu et al. 2011a, b). To address the quantitative 3D model, we quantify the 3D depositional character of the study area based on a series of typical stratal slices for each MSC unit (Fig. 16 right). During the MSC1–7 sedimentary deposition stage, a long-term base-level fall cycle, with  $A/S < 1$ , has developed fastly progradation delta front subfacies in the study area because of strong sedimentary supply and the limit of accommodation space, the Dongying Delta is the dominating facie in the central part of Dongying Depression associated with relative stable tectonic movement (Zhang et al. 1997; Lin et al. 2003). As for the details, the underwater distributary channel mainly develops along the EW direction. During the MSC8–14 sedimentary deposition stage, a long-term base-level rise cycle, with  $A/S > 1$ , has developed slowly retrogradation delta plain subfacies in the study area because of less sedimentary supply and abundant accommodation space, the Dongying delta bypasses the central part of the Dongying Depression associated with relative stable tectonic movement (Zhang and Ji 1997; Liu et al. 2014). Moreover, the direction of sedimentary source in the delta plain is EW orientation. Furthermore, the thickness of the upper and lower part of the second member of the Shahejie Formation is the same based on the quantitative statistics.

## Conclusion

The results of this research can be summarized as follows:

- (1) Based on the analysis of well logs, core, and seismic data, the second member of the Shahejie Formation can be divided into two long-term base-level cycle. Furthermore, the long-term base-level cycle can be classified into 14 middle-term base-level cycles (MSC1–14).
- (2) During the second member of the Shahejie Formation in the study area, the characteristics of sedimentary system are as follows: (i) coarse-to-fine sandstone interbedded with abundant mudstone and shale; (ii) upward-fining interval in delta plain deposit and upward-coarsening interval in delta front deposit; (iii) mouth bar with medium-fine sandstone, massive bedding, and funnel-shaped log curve; (iv) channel with medium-coarse sandstone, wedge-shaped cross-bedding, and bell-shaped log curve.
- (3) The sedimentary systems can be further divided into two subfacies (namely delta plain and delta front) and five microfacies (namely distributary channel, inter-channel, underwater distributary channel, mouth bar, and tributary bay). During the deposition stage of MSC1–7, the channel mainly develops at EW direction with progradation patterns. And during the deposition stage of MSC6–7, the mouth bar develops at the central part of the study area with maximum 1.5 km<sup>2</sup>. As for the deposition stage of MSC8–14, the channel also mainly develops in EW direction with a retrogradation pattern.
- (4) Upon the elaborate analysis of 3D sedimentary system in the study area, during the MSC1–7, the delta front is rapidly generated with  $A/S < 1$ . On the other hand, during the MSC8–14, the delta plain is slow-growth with  $A/S > 1$ .

**Acknowledgements** The authors would like to thank Geoscope Software Company for providing the software to make an interpretation. Particularly, thanks are due to the Shengli Oilfield Company for using the recent 3D seismic data, core, and well data. Also, the authors thank Zili Zhang for his viewpoint about the interpretation about the background and the reviewers' comments.

**Funding information** The research is supported by the National Science and Technology Major Project (No. 2017 Z X 05001-002).

## References

- Allen MB, Macdonald DIM, Zhao X et al (1997) Early Cenozoic two-phase extension and late Cenozoic thermal subsidence and inversion of the Bohai Basin, Northern China. *Mar Pet Geol* 14(7):951–972
- Catuneanu O, Abreu V, Bhattacharya JP, Blum MD, Dalrymple RW, Eriksson PG, Fielding CR, Fisher WL, Galloway WE, Gibling MR, Giles KA, Holbrook JM, Jordan R, Kendall CGSC, Macurda B, Martinsen OJ, Miall AD, Neal JE, Nummedal D, Pomar L, Posamentier HW, Pratt BR, Sarg JF, Shanley KW, Steel RJ, Strasser A, Tucker ME, Winker C (2009) Towards the standardization of sequence stratigraphy. *Earth Sci Rev* 92(1–2):1–33
- Cross TA (1988) Controls on coal distribution in transgressive-regressive cycles, Upper Cretaceous, Western Interior, U. S. A. In: Wilgaus CK et al (eds) *Sea-level changes: an integrated approach*, SEPM Special Publication, vol 42(1), pp 371–380
- Curry MAE, Peel FJ, Hudec MR, Norton IO (2018) Extensional models for the development of passive-margin salt basins, with application to the Gulf of Mexico. In: *Basin Res*, vol 30, pp 1180–1199. <https://doi.org/10.1111/bre.12299>
- Dong Y, Zhu X, Xian B, Cheng K, Wang P (2014) Mapping sediment-dispersal characteristics using seismic geomorphology: late Paleogene to Neogene, Qinan Sag, Huanghua Depression, China. *Mar Petrol Geol* 54(2):180–197
- Dong Y, Zhu X, Xian B, Hu T, Geng X, Liao J, Luo Q (2015) Seismic geomorphology study of the Paleogene Hetaoyuan Formation, central-south Biyang Sag, Nanxiang Basin, China. *Mar Geol* 64: 104–124
- Feng YL (1999) Lower tertiary stratigraphy framework and basing filling model in Dongying depression (in Chinese with English abstract). *Oil Gas Geol* 14(3):173–179
- Feng YL, He LK, Zheng HR et al (1990) Gravity flow deposits of prodelta slope from third member of Shahejie Formation, Niuzhuang region, Shangdong province (in Chinese with English abstract). *Oil Gas Geol* 11(3):313–319
- Feng Y, Li S, Lu Y (2013) Sequence stratigraphy and architectural variability in Late Eocene lacustrine strata of the Dongying Depression, Bohai Bay Basin, Eastern China. *Sediment Geol* 295(8):1–26
- Flemming BW (2007) The influence of grain-size analysis methods and sediment mixing on curve shapes and textural parameters: implications for sediment trend analysis. *Sediment Geol* 202(3):425–435

- Galloway WE (1989) Genetic stratigraphy sequences in basin analysis I: architecture and genesis of flooding-surface bounded depositional units. *Am Assoc Petrol Geol* 73:125–142
- Lin CS, Zheng HR, Ren JY et al (2003) The control of syn-depositional faulting on the Eocene sedimentary basin fills of the Dongying and Zhanhua Sags, Bohai Bay Basin (in Chinese with English abstract). *Science China Ser D* 33(11):1025–1036
- Liu J, Jian X, Kang B et al (2014) Paleogeomorphology of the middle part of third member of the Shahejie Formation and their effects on depositional systems, Dongying Delta, Dongying Depression (in Chinese with English abstract). *Pet Geol Recover Effic* 21(1):20–23
- Reading HG, Collinson JD (1996) River deltas. In: *Sedimentary environments: processes, facies and stratigraphy*. Blackwell Publishing Company, Malden, pp 688–696
- Ren J, Tamaki K, Li S et al (2002) Late Mesozoic and Cenozoic rifting and its dynamic setting in Eastern China and adjacent areas. *Tectonophysics* 344(3–4):175–205
- Smit FWH, van BFSP, Holst JC et al (2018) Seismic geomorphology and origin of diagenetic geobodies in the Upper Cretaceous Chalk of the North Sea Basin (Danish Central Graben). *Basin Res*. <https://doi.org/10.1111/bre.12285>
- Vail PR, Mitchum RM Jr, Todd RG, et al (1997) Seismic stratigraphy and global changes of sea level. In: Payton CE (ed) *Seismic stratigraphy*. *Am Assoc Petrol Geol Mem* 26(4):49–212
- Wang J (2005) Sedimentary facies of the Shahejie Formation of Paleogene in Dongying Sag, Jiyang Depression (in Chinese with English abstract). *J Paleogeogr* 7(1):45–58
- Wu J, Zhang Z, Wang B (2000) The key boundaries of sequence stratigraphy and their correlative affair in Inland Depressions: an example from the second member and the upper part of the third member of the Shahejie Formation in Dongying Depression (in Chinese with English abstract). *J Stratigr* 24(1):78–83
- Xie X, Bethke CM, Li S, Liu X, Zheng H (2001) Overpressure and petroleum generation and accumulation in the Dongying Depression of the Bohaiwan Basin, China. *Geofluids* 1(1):257–271
- Zeng H, Hentz TF (2004) High-frequency sequence stratigraphy from seismic sedimentology: a Miocene Gulf Coast example. *AAPG Bull* 88(2):153–174
- Zeng H, Henry SC, Riola JP et al (1998) Stratal slicing: part II. Real seismic data. *Geophysics* 63(2):514–522
- Zhang S, Ji Y (1997) The control of Paleogene climate on sequence stratigraphy in Dongying Depression (in Chinese with English abstract). *J Univ Pet China* 22(6):26–30
- Zhang R, Yu S, Wu J (1997) The effect of sediments supply condition on sequence stratigraphy analysis in continental lacustrine basins (in Chinese with English abstract). *Earth Sci J China Univ Geosci* 22(2):139–143
- Zhen Z, Liu Z, Sun P et al (2012) Grain size analysis and contrast between fan delta and underwater fan in Eocene Huadian Formation in Huadian Basin (in Chinese with English abstract). *Glob Geol* 31(4):681–692
- Zhou L, Cao Y (2010) The application of clastic grain size analysis to the genetic study of sand bodies in Upper Es4 Submember of Xin176 area in Dongying Sag. *Acta Geosci Sin* 31(4):563–573
- Zhu H, Yang X, Zhou X et al (2011a) High resolution three-dimensional facies architecture delineation using sequence stratigraphym, seismic sedimentology: example from Dongying Formation in BZ 3-1 Block of Western slope of Bozhong Sag, Bohai Bay Basin (in Chinese with English abstract). *Earth Sci J China Univ Geosci* 36(6):1073–1084
- Zhu X, Dong Y, Hu T et al (2011b) Seismic sedimentology study of fine sequence stratigraphic framework: a case study of the Hetaoyuan Formation in the Biyang Sag (in Chinese with English abstract). *Oil Gas Geol* 32(4):615–624
- Zong GH, li CB, Xiao HQ (1999) Evolution of Jiyang Depression and its tectonic implications (in Chinese with English abstract). *Geol J China's Univ* 5(3):275–282